P2.24

GENERATION OF TURBULENCE WITHIN AN UPPER-TROPOSPHERIC FRONT

Steven E. Koch[1], Melvyn A. Shapiro[2], Brian Jamison[1], Ed Tollerud[1], and Tracy Smith[1]

[1] *NOAA Research – Forecast Systems Laboratory, Boulder,Colorado*
[2] *NOAA Research – Environmental Technology Laboratory*

1. Introduction

The generation of clear-air turbulence (CAT) is generally thought to be the product of vertical shear instability arising in thin sheets of the atmosphere. Operational model guidance for forecasting CAT uses a fuzzy logic approach applied to a multitude of algorithms computed from the Rapid Update Cycle (RUC) model (Sharman et al. 1999). All of these algorithms are based on some application of the shearing instability principle or the associated Turbulent Kinetic Energy (TKE) generation concept. Recent research conducted at the Forecast Systems Laboratory has shown that CAT also occurs in diagnosed regions of unbalanced flow associated with the jet stream, not collocated with the regions of diagnosed TKE generation (Koch and Caracena 2002). Gravity-inertia waves diagnosed in surface mesoanalyses are generated in regions of imbalance (Koch and O'Handley 1997; Koch and Saleeby 2001). It is unclear why gravity waves should relate to observed reports of moderate-or-greater (MOG) turbulence, since such waves display wavelengths that are much longer than the ~ 1 – 5 km Kelvin-Helmholtz waves generated by shearing instability. Observations of gravity wave-turbulence interactions near the upper-level jet are very much needed.

The Severe Clear Air Turbulence Colliding with Aircraft Traffic (SCATCAT) experiment was conducted in the winter of 2001 over the Pacific Ocean to test the performance of RUC model predictors of turbulence and to improve understanding of turbulence generation mechanisms. The NOAA Gulfstream-IV (G-IV) aircraft collected flight-level and dropsonde data in a region extending from the core of an intense upper-level jet to its left exit region on 17-18 February 2001 (Fig. 1). During the aircraft mission, 25-Hz measurements were made from a stack of constant-altitude legs taken nearly perpendicular to the jet streak at altitudes of 12.5, 11.3, 10.7, and 10.1 km and dropsondes were launched at ~ 40-km intervals from the 12.5 km level. In addition, the RUC model was run on a 20-km grid with 50 hybrid isentropic-sigma levels in a manner closely mirroring the operational RUC model. The only exception was that the domain was shifted to the data-sparse central north Pacific and the AVN model supplied the RUC with boundary conditions instead of the Eta model. The dropsonde and in-flight data and the model fields were used to investigate for the first time the interrelationships among the observed and simulated gravity waves, upper-level frontal structure, and dropsonde-diagnosed turbulence.

Corresponding author address: Steven E. Koch, NOAA/OAR/FSL, FS1, 325 Broadway, Boulder, CO 80305-3328; e-mail < Steven.Koch@noaa.gov>

2. Tropopause undulations, mesoscale gravity waves, and turbulence

The RUC model produced a rather deep tropopause fold within an upper-level frontal zone on the cyclonic side of the jet streak (Fig. 2). Also, several tropopause undulations can be seen in the model fields, as well as mesoscale gravity waves directly above these undulations. The horizontal wavelength of these vertically propagating gravity waves varies with height from 160–260 km. The waves propagated away from the local tropopause undulation areas. Cross-section analyses computed from the dropsonde data (Fig. 3) also show vertically propagating mesoscale gravity waves in the region of strong vertical wind shear extending from the jet core (and its cyclonic side) into the lower stratosphere.

The DTF3 turbulence diagnostic algorithm (Marroquin 1998) applied to the dropsonde data (Fig. 3) indicates coherent streaks of MOG turbulence principally in three regions: the layer of strong vertical shear above the jet core, the shear layer directly beneath the jet core, and within the region of strong shear and stability along the warm frontal zone. The G-IV did, in fact, encounter MOG turbulence in the uppermost of these regions on the three lower legs of the stack (yellow parts of the black flight segments). Diagnosed MOG turbulence from the RUC model appears in the same general regions (Fig. 4). The strong association between the tropopause undulations, the gravity waves, and both detected and diagnosed turbulence above the jet is striking.

The diagnosed TKE (the DTF fields) in the RUC simulation appear as mesoscale bands at 33, 35, 37, and 39 Kft (Fig. 5). The bands are parallel to the general northwesterly wind regime and frontal structure (isotherms) at these altitudes and occur in the cyclonic exit region of the upper-level jet. These bands developed with time in the model forecast. The

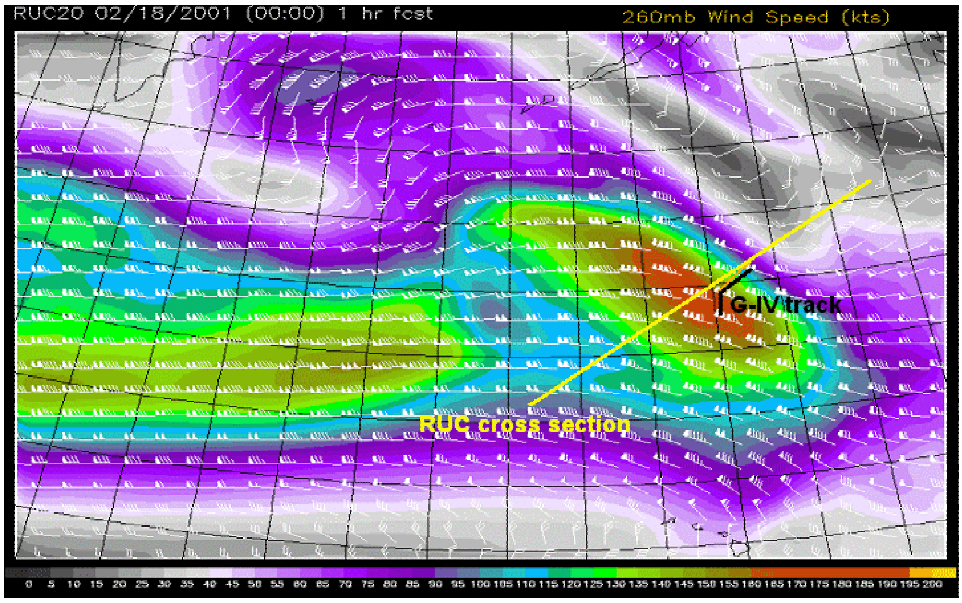

Fig.1 RUC 1-h forecast of 33 000 ft (260 mb) isotachs and wind barbs at 0000 UTC 18 February 2001 over the Pacific Ocean (note Hawaiian Islands and Aleutian Islands). Forecast maximum jet winds are 92 m s^{-1} vs. 100 m s^{-1} observed by the G-IV aircraft. Locations of RUC and G-IV vertical cross sections shown below are also depicted.

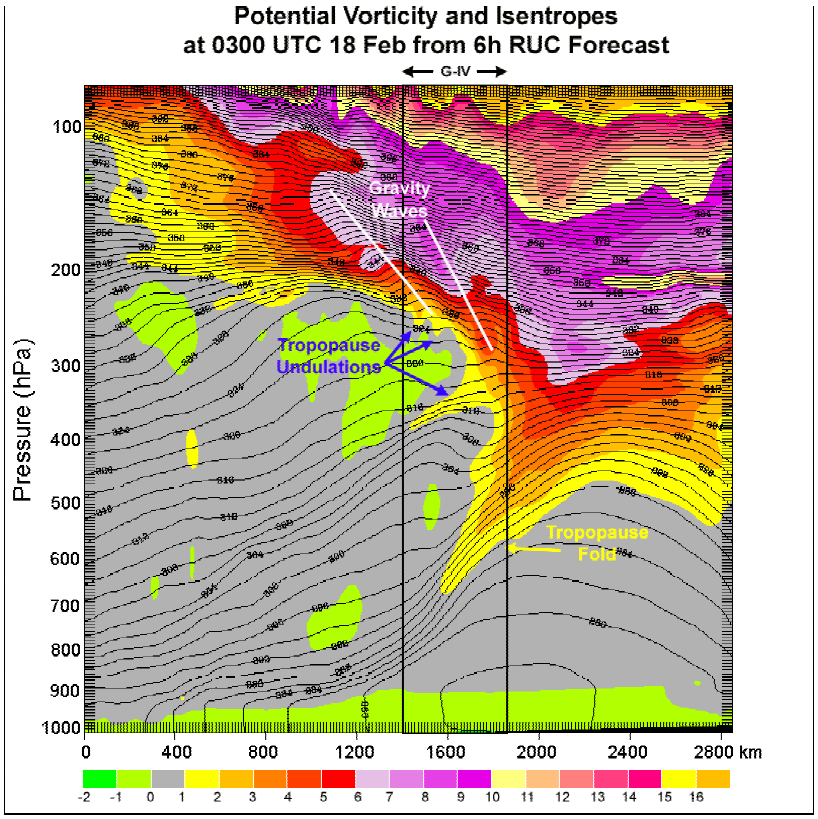

Fig.2 Isentropic cross section of RUC 6-h forecast isentropic potential vorticity and potential temperature valid at 0300 UTC 18 February 2001. Parallel vertical lines denote segment over which G-IV aircraft took measurements, and for which the cross section in Fig. 3 is relevant. Note deep tropopause fold (>1.5 PVU) and several tropopause undulations, above which occur vertically propagating gravity waves.

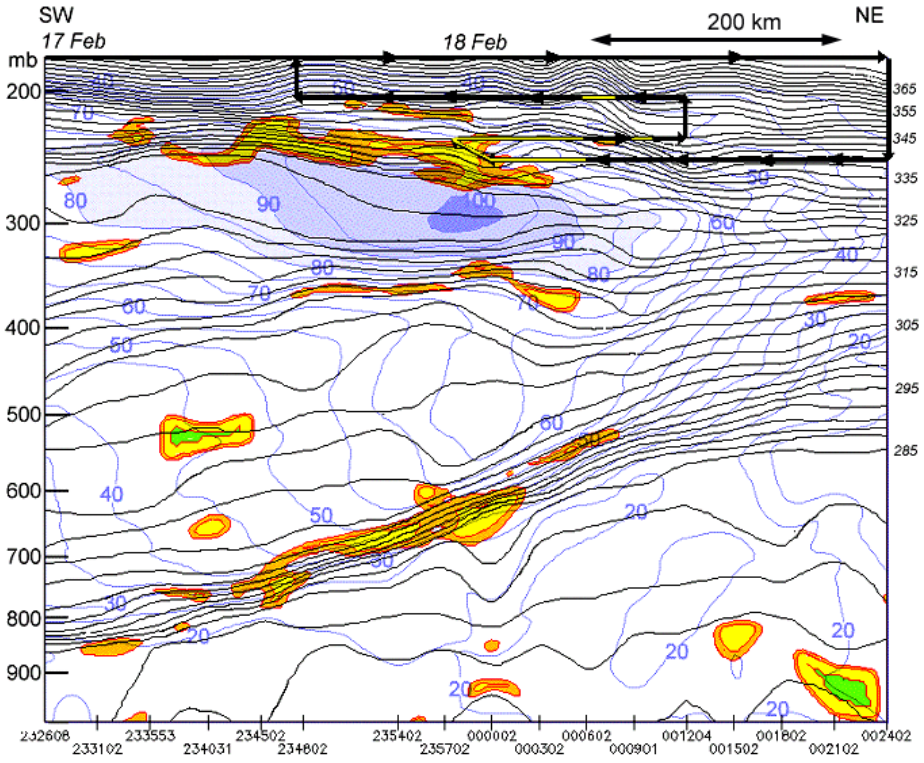

Fig.3 Vertical cross section of wind magnitude (blue lines, 5 m s^{-1} isotachs), potential temperature (black lines, 2K isentropes), and DTF3 turbulence diagnostic computed from dropsondes (note release times at bottom of display) from 232606 UTC 17 February through 002402 UTC 18 February 2001. Jet core is highlighted by winds in excess of 80 m s^{-1} (maximum of 100 m s^{-1}), and DTF3 values are contoured at 0.6 and 1.0 m^2 s^{-3} (yellow and orange areas, respectively). Also shown are the four stacked legs of the G-IV tracks (black lines with arrows depicting sense of aircraft travel), and those segments of the legs (yellow highlighting) for which moderate-or-greater turbulence was diagnosed in the flight-level data (see text). Note distance scale at top of display. Compare this analysis with those derived from the RUC model forecasts in Figs. 2 and 4.

dynamical cause for this banded behavior is under investigation currently.

3. Ozone, forecast potential vorticity fluctuations, and gravity waves

Comparisons were made between flight-level time series observations and fields analyzed from the RUC model simulation. The method for deriving model "meteograms" consisted of three steps. First, the three-dimensional model grid data were interpolated to the plane of the cross section at 10-km intervals. Next, the 25-mb resolution model data were vertically interpolated to the constant-height altitudes flown by the aircraft. Finally, a space-to-time conversion was performed under the assumption of stationarity for the duration of each flight leg.

Potential vorticity is a surrogate for ozone, since both are conserved quantities acting as passive tracers of stratosphere-troposphere air mass exchange processes. Extreme ozone fluctuations from 300 to >800 ppbv were measured by the G-IV at 41Kft (175 mb, which is above the jet core), as the aircraft penetrated the gravity waves above the tropopause undulations (Fig. 6). Fluctuations in the RUC potential vorticity "meteogram" do not relate well to ozone variability seen in the aircraft observations at this altitude. Considerable variability in the potential temperature observations was also present, and did not correlate well with the ozone data, nor was MOG turbulence reported on this flight leg. We conclude that these rapid fluctuations in ozone at this level represent "fossil turbulence" or remnants of earlier stratosphere-troposphere turbulent exchange processes.

By contrast, the correlation between the variability in ozone and RUC potential vorticity and potential temperature data is quite high at the lowest (33 Kft , or 260 mb) level (Fig. 7). Note the general decrease of both conservative quantities as one progresses from the cyclonic side of the jet at 0030 UTC back to the jet core by 0055 UTC. Examination of the dropsonde cross-section analysis (Fig. 3) reveals that the aircraft was penetrating a rather pronounced gravity wave within the upper-tropospheric frontal zone at this level immediately to the right (northeast) of the high TKE region. MOG turbulence was detected by the aircraft beginning at 0047 UTC (Fig. 7). Close inspection of the G-IV time series in Fig. 7 suggests that very high-frequency energy begins to appear at about this time. Spectral

analyses of the aircraft data confirmed that MOG turbulence did, in fact, begin then within this gravity wave system. Phase spectrum analyses showed that potential temperature and the jet-normal wind component exhibited a strong in-phase relationship, indicating the presence of either deep propagating gravity waves or possibly, decaying (evanescent) waves.

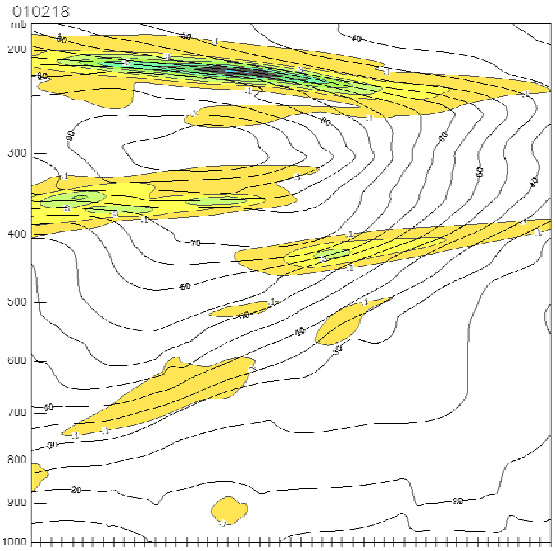

Fig. 4 Diagnosed turbulence in RUC initial analysis at 0000 UTC 18 February using the DTF5 algorithm (shaded regions) and wind speed (5 m s^{-1} isotachs).

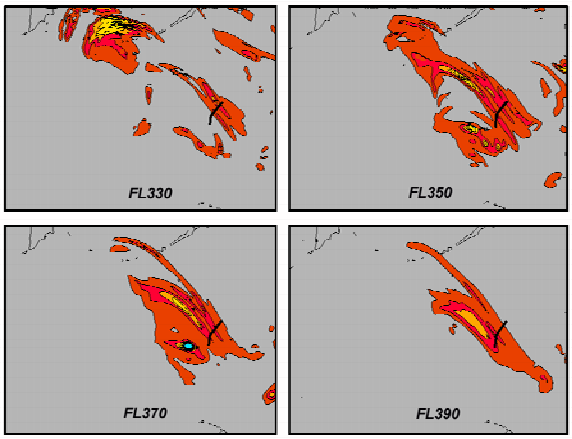

Fig. 5 Altitude variation of DTF3 forecast by RUC for 0300 UTC (6-h forecast). Shown are the fields at 33, 35, 37, and 39 Kft altitudes over the full model domain (note the Aleutian Islands to the north and the Hawaiian Islands to the south). The G-IV track is depicted by small, thick black line segment.

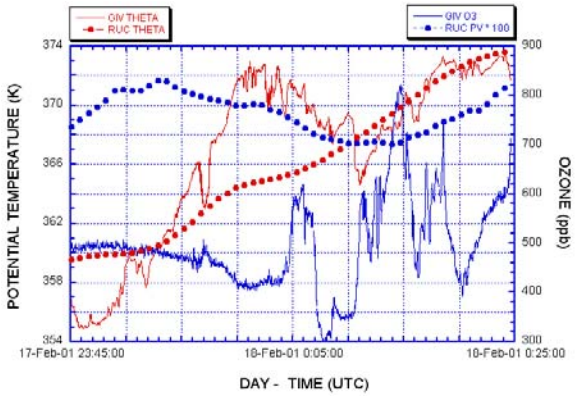

Fig. 6 Comparisons between in-flight measurements and RUC forecast of potential temperature at 41 Kft (red curve and red dots, respectively) for the period 2345 UTC 17 February–0025 UTC 18 February. In-flight measurements of ozone (blue curve) are also compared to RUC potential vorticity (blue dots). RUC values are computed using the meteogram technique described in the text.

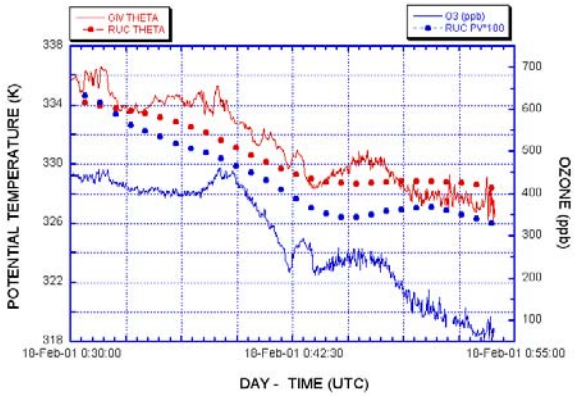

Fig. 7 As in Fig. 6 except for 33 Kft level for the period 0030–0055 UTC 18 February. Potential vorticity values are multiplied by 100, so values >150 are stratospheric in nature. The largest-scale fluctuations in the G-IV data are the mesoscale gravity waves with horizontal wavelengths ~100 km.

4. Conclusions

Synthesis of in-flight data, dropsonde data, and RUC model analyses leads to the conclusion that MOG turbulence occurred in conjunction with gravity waves shed from within the upper-level frontal zone on the cyclonic shear side of the jet core. Two- and three-dimensional numerical modeling studies (Reeder and Griffiths 1996; Koch 2001; Zhang et al. 2001) lend support to the idea that upper-level frontal zones are prolific producers of gravity-inertia waves. The relationships between ozone and potential vorticity fluctuations, observed and simulated gravity waves, and turbulence in the present case suggests that upward-propagating gravity waves are generated above mesoscale undulations in the tropopause, and that local

enhancement of the shear by the waves may be the causative factor in the generation of turbulence at smaller scales. In particular, spectral analyses show that turbulence related to energetic fluctuations in the inertial subrange occurred within a packet of non-monochromatic gravity waves with wavelengths of 6 – 80 km. The challenge now is to attempt to model and understand these features using a properly initialized cloud-resolving model.

5. Acknowledgments

This research is in response to requirements and funding by the Federal Aviation Administration (FAA). The views expressed are those of the authors and do not necessarily represent the official policy or position of the FAA. The efforts of Cecilia Girz to coordinate the field phase of this project are gratefully acknowledged.

6. References

Koch, S. E., 2001: Status report on the predictability of mesoscale gravity waves with numerical weather prediction models. Preprints, *9th Conference on Mesoscale Processes,* Ft. Lauderdale, FL, Amer. Meteor. Soc., 264-268.

Koch, S. E., and S. Saleeby, 2001: An automated system for the analysis of gravity waves and other mesoscale phenomena. *Wea. Forecasting*, **16,** 661-679.

Koch, S. E., and C. O'Handley, 1997: Operational forecasting and detection of mesoscale gravity waves. *Wea. Forecasting*, **12,** 253-281.

Koch, S. E., and F. Caracena, 2002: Predicting clear-air turbulence from diagnosis of unbalanced flow. Preprints, *10th Conference on Aviation, Range, and Aerospace Meteorology*, Portland, OR, Amer. Meteor. Soc., 359-363.

Marroquin, A., 1998: An advanced algorithm to diagnose atmospheric turbulence using numerical model output. Preprints, *16th Conf. on Weather Analysis and Forecasting*, Phoenix, AZ, American Meteor. Society, 79-81.

Reeder, M. J., and M. Griffiths, 1996: Stratospheric inertia-gravity waves generated in a numerical model of frontogenesis. Part I: Wave sources, generation mechanisms and momentum fluxes. *Quart. J. Roy. Met. Soc.,* **122,** 1175-1195.

Sharman, R.C., C. Tebaldi, and B. Brown, 1999: An integrated approach to clear-air turbulence forecasting. Preprints, *8th Conf. on Aviation, Range, and Aerospace Meteorology*, Dallas, TX, Amer. Meteor. Soc., 68-71.

Zhang, F., S. E. Koch, C. A. Davis, and M. L. Kaplan, 2001: Wavelet analysis and the governing dynamics of a large-amplitude mesoscale gravity wave event along the East Coast of the United States. *Quart. J. Roy. Meteor. Soc.,* **127,** 2209-2245.